• Basic Research •

Integrated single-cell and Mendelian randomization analyses prioritize immune-related candidate genes and pathways in proliferative diabetic retinopathy

Ying Gao[1,2], *Feng Yan*[3], *Jing-Fan Wang*[1], *Jiao-Yu Deng*[4], *Peng-Fei Ge*[1], *Yi-Fan Lin*[1], *Yang-Yang Lu*[1], *Hai-Yue Xie*[1], *Zi-Zhong Hu*[1], *Ping Xie*[1]

[1]Department of Ophthalmology, the First Affiliated Hospital of Nanjing Medical University, Nanjing 210029, Jiangsu Province, China
[2]Department of Ophthalmology, Sir Run Run Hospital, Nanjing Medical University, Nanjing 211112, Jiangsu Province, China
[3]Department of Ophthalmology, Taikang Xianlin Drum Tower Hospital, Affiliated Hospital of Medical School, Nanjing University, Nanjing 210046, Jiangsu Province, China
[4]Department of Ophthalmology, the Affiliated Jiangning Hospital of Nanjing Medical University, Nanjing 211000, Jiangsu Province, China
Co-first Authors: Ying Gao and Feng Yan
Correspondence to: Zi-Zhong Hu and Ping Xie. Department of Ophthalmology, the First Affiliated Hospital of Nanjing Medical University, Nanjing 210029, Jiangsu Province, China. huzizhong@njmu.edu.cn; xieping9@njmu.edu.cn
Received: 2026-08-31 Accepted: 2026-10-19

Abstract

● **AIM:** To prioritize immune-related candidate genes and pathways, elucidate immune dysregulation mechanisms, and provide potential therapeutic targets for diabetic retinopathy (DR).

● **METHODS:** Single-cell RNA sequencing (scRNA-seq) analysis was performed using fibrovascular membranes (FVMs) obtained from patients with proliferative diabetic retinopathy (PDR) and from normal retinas. Differentially expressed genes (DEGs) were identified by comparing FVMs to normal retinas, followed by gene set enrichment analysis (GSEA) to characterize immune-related pathways enriched in cell populations. Additionally, Mendelian randomization (MR) analysis was performed to explore the causal associations between immune cell traits and PDR. By integrating single-nucleotide polymorphism (SNP)-annotated genes with PDR scRNA-seq profiles, intersection analysis was performed to prioritize key genes within pathways enriched in PDR major cell populations through MR analysis. The prioritized candidate genes were subsequently validated in human retinal endothelial cells (hRECs) and human monocytic leukemia cell line (THP-1) cells, which were exposed to inflammatory condition.

● **RESULTS:** scRNA-seq analysis demonstrated that the major cell populations within FVMs from patients with PDR consisted of macrophages, monocytes, T cells, B cells, retinal vascular endothelial cells, fibroblasts, and pericytes. MR analysis prioritized two immune-cell traits as potential risk factors for PDR, including CD8 on CM CD8br [odds ratio (OR)=1.077, 95%CI: 1.017–1.140] and HLA DR on $CD14^{+}CD16^{-}$ monocytes (OR=1.079, 95%CI: 1.034–1.126); instrumental SNPs for the two prioritized immune traits were located near genes, including CD8 on CM CD8br (*ZMAT4*, *ZBTB16*, *PIP5K1B*, and *CD8A*) and HLA DR on $CD14^{+}CD16^{-}$ monocytes (*GLI2*, *KATNIP*, *LYZ*, *ERBB4*, *UQCC2*, *WDR72*, *RYR2*, *ZNF442*, and *FLJ12825*). Among these, *CD8A* mapped to the HALLMARK_ALLOGRAFT_REJECTION pathway, which was enriched in the major cell populations within FVMs from patients with PDR. Overlap analysis of genes within this pathway across major cell populations prioritized six overlapping candidate genes (*CTSS*, *STAT1*, *B2M*, *CD74*, *CCL2*, and *TIMP1*), among which *CTSS* was shared across all six cell types. Quantitative real-time polymerase chain reaction assays in an *in vitro* inflammatory microenvironment model of DR showed that *CTSS* expression was significantly upregulated in lipopolysaccharide (LPS)-stimulated THP-1 cells; however, no significant difference was observed in hRECs.

● **CONCLUSION:** This study prioritizes immune-related candidate genes and pathways potentially involved in PDR pathogenesis, providing exploratory value for further investigation.

● **KEYWORDS:** proliferative diabetic retinopathy; immune cells; single-cell sequencing; Mendelian randomization
DOI:10.18240/ijo.2026.12.04

Citation: Gao Y, Yan F, Wang JF, Deng JY, Ge PF, Lin YF, Lu YY, Xie HY, Hu ZZ, Xie P. Integrated single-cell and Mendelian randomization analyses prioritize immune-related candidate genes and pathways in proliferative diabetic retinopathy. *Int J Ophthalmol* 2026;19(12):2337-2349

INTRODUCTION

Diabetic retinopathy (DR), a common ocular complication of diabetes, represents a major contributor to blindness, with its age-standardized prevalence increasing globally between 1990 and 2020. The global diabetic population is projected to surpass 600 million by 2040, accompanied by a substantial increase in the prevalence of DR and related visual impairment[1]. DR exhibits a progressive clinical course, developing from non-proliferative diabetic retinopathy (NPDR) to proliferative diabetic retinopathy (PDR). Current therapeutic approaches mainly comprise retinal laser photocoagulation, vitrectomy, and intravitreal injection of anti-vascular endothelial growth factor (VEGF). Nevertheless, these interventions have several limitations: laser photocoagulation may induce irreversible retinal injury[2], anti-VEGF therapy requires repeated injections to maintain efficacy[3], and rapid recurrence of retinopathy may occur following treatment discontinuation[4]. Consequently, the healthcare and socioeconomic burden associated with DR continues to escalate. Therefore, accurate prioritization of sensitive candidate genes and pathways for DR and the establishment of more effective therapeutic strategies remain important objectives for improving patient outcomes.

Mendelian randomization (MR) employs genetic variants as instrumental variables (IVs) to assess potential causal relationships between exposure factors and outcome variables, with genetic variant information derived from non-experimental studies. In recent years, MR has become an increasingly valuable approach for causal inference, as it leverages genetic variants to estimate causal effects between exposures and outcomes while reducing the influence of confounding factors frequently present in conventional epidemiological investigations[5]. Single-cell RNA sequencing (scRNA-seq) is a sophisticated molecular profiling approach that allows for the characterization and isolation of distinct cellular populations at the single-cell level. The development of scRNA-seq has overcome limitations associated with cellular heterogeneity in complex biological samples, allowing precise identification of diverse cell subpopulations and comprehensive analysis of cellular differentiation trajectories and regulatory signaling networks. This technology offers a thorough insight into the molecular features of individual cells within biological systems and their roles in disease progression. Therefore, scRNA-seq has been extensively adopted in both basic and clinical research fields[6].

Some studies have employed MR analysis to investigate the potential causal relationship between cheese intake and the risk of DR[7]. Growing evidence suggests that immune system activation serves a pivotal function in DR progression[8]. Single-nucleotide polymorphisms (SNPs) served as IVs in MR analyses to investigate potential causal relationships between immune cell characteristics and DR. These investigations have suggested that monocytes and T cells may represent promising therapeutic targets for DR management[9-10]. Recently, scRNA-seq has been extensively applied to characterize gene expression patterns and define cellular populations within fibrovascular membranes (FVMs) from patients with PDR. This approach identified five major cell populations, including macrophages, monocytes, B cells, $CD8^+$ T cells, and fibroblasts. Moreover, CellChat analysis demonstrated potential cell-cell interactions between $CD8^+$ T cells and macrophages[11].

Currently, inflammation is considered a major pathogenic mechanism underlying DR development and is closely linked to M1 macrophage polarization[12]. Classical ($CD14^+CD16^-$) monocytes are essential mediators of the early inflammatory response, with the capacity to differentiate into macrophages within tissues and promote chronic disease progression[13]. Previous studies have indicated that $CD8^+$ T cells are actively involved in the inflammatory processes associated with DR[14]. Collectively, these findings suggest that M1 polarization, monocytes, and $CD8^+$ T cells contribute to PDR pathogenesis through complex intercellular interactions. The present study integrates MR analysis of these three immune cells populations with scRNA-seq data obtained from FVMs of patients with PDR to prioritize novel immune-related candidate genes and pathways associated with the diagnosis and treatment of PDR (Figure 1).

MATERIALS AND METHODS

Ethical Approval All data were obtained from publicly available databases, and all experimental procedures were performed using commercially available cell lines.

Data Source scRNA-seq datasets were procured from the Gene Expression Omnibus (GEO) database (https://www.ncbi.nlm.nih.gov/geo/). A scRNA-seq dataset comprising 6335 cells derived from FVMs of five patients with PDR was obtained from GEO (GSE165784). Additionally, 18 075 cells from normal retinal tissues of two patients without DR were collected from the GEO database (GSE188280). The number of donors and cells contributed by each donor were reported. For outcome variables, publicly available genome-wide association study (GWAS) summary data from the FinnGen database were utilized to identify a PDR-related dataset: finngen_R9_DM_RETINA_PROLIF (https://www.finngen.fi/). For exposure variables (immune cells), 731 immune cell

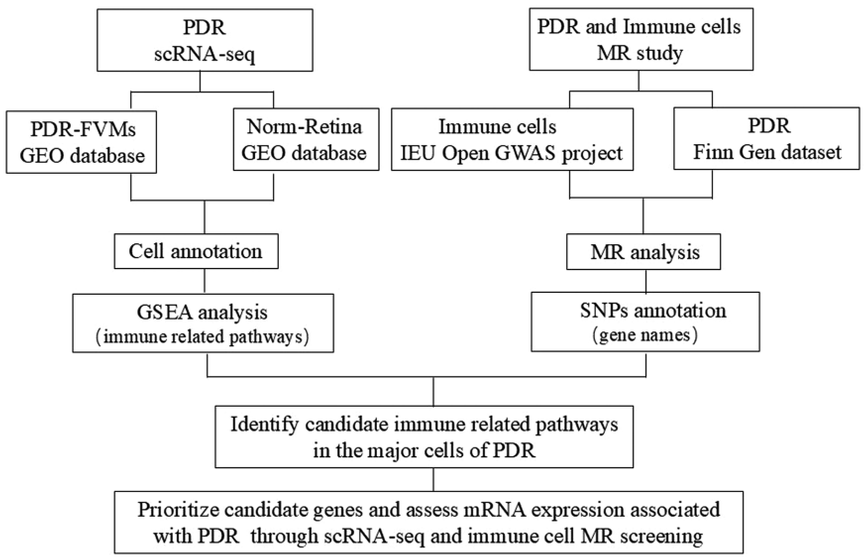


Figure 1 Flowchart of the entire analysis PDR: Proliferative diabetic retinopathy; MR: Mendelian randomization; FVM: Fibrovascular membranes; SNP: Single-nucleotide polymorphism; scRNA-seq: Single-cell RNA sequencing; GSEA: Gene set enrichment analysis; GEO: Gene Expression Omnibus; GWAS: Genome-wide association study; IEU Open GWAS project: MRC Integrative Epidemiology Unit Open GWAS project.

datasets were procured from the IEU GWAS database (https://gwas.mrcieu.ac.uk/), all immune trait GWAS were likewise of European ancestry. Previous research has demonstrated that M1 macrophages, monocytes, and $CD8^+$ T cells are closely involved in PDR pathogenesis. Among the 731 immune cell traits examined, monocytes[13] and $CD8^+$ T cells[15-17] were reported to be strongly associated with M1 macrophage polarization. Therefore, these immune cell populations were selected as exposure factors.

Processing of Single-Cell RNA-seq Data

Single-cell sequencing data analysis scRNA-seq data underwent analysis *via* the Seurat package in R. Quality control was performed according to three filtering criteria: fewer than 3000 filtered genes, more than 200 filtered genes, and a mitochondrial gene proportion below 20% per cell. Subsequently, gene expression values underwent normalization *via* the NormalizeData function. The FindVariableFeatures and ScaleData functions were applied to identify the top 2000 most variable features and perform data scaling, while regressing out the dataset (with total number of RNA counts and percent mitochondria regressed out). The RunHarmony function was applied to correct batch variations introduced during the integration of multi-sample single-cell sequencing datasets. Subsequent dimensionality reduction and clustering analyses were executed utilizing the RunPCA, FindNeighbors, FindClusters, and RunUMAP functions with default parameters. Cell populations were annotated using single R and established retinal marker genes. scRNA-seq analysis was conducted to dissect the cellular composition in FVMs, with normal retinal scRNA-seq datasets serving as a reference baseline. Cluster markers used for cell-type annotation were identified using the FindAllMarkers function in the Seurat software package with thresh. use=0.25 and min.pct=0.25[18]. Differentially expressed genes (DEGs) analysis between PDR and control samples was performed using a donor-level pseudobulk strategy to reduce pseudoreplication bias.

Single cell annotation Cell types were identified according to expression profiles of established marker genes. Astrocytes were annotated by *GFAP* expression; macrophages were identified by *CD68* and *CD163* expression; monocytes were characterized by *CD14* and *FCGR3A* expression; vascular endothelial cells were defined according to *VWF* and *CLDN5* expression; B cells were identified by *CD79A* expression; T cells were annotated using *CD3E*, *CD8A*, and *CD3G* expression; fibroblast pericytes were identified based on *THY1*, *COL1A1*, and *RGS5* expression. Neurons were classified according to *OTX2* expression. Additionally, the R package SingleR was applied as a reference tool for validating cell cluster annotation.

Pathway enrichment analysis DEGs were identified by comparing FVMs to normal retinas, and pathway enrichment profiles in DEGs were evaluated *via* gene set enrichment analysis (GSEA). Hallmark pathway gene sets were procured from the Molecular Signatures Database. The criteria applied for GSEA significance were defined as follows: normalized enrichment score (NES) >1.0; false discovery rate (FDR) Q-value<0.25; nominal P<0.05.

Processing of MR Data

Selection and validation of IVs Exposure and outcome GWAS summary statistics were harmonized utilizing the harmonise_data( ) function implemented in the TwoSampleMR

R package. This procedure automatically aligned effect alleles between exposure and outcome datasets. MR analyses were performed using multiple approaches, including simple mode, weighted mode, weighted median, inverse variance weighting (IVW), and MR-Egger regression, to examine potential causal associations between immune cells and PDR. IVW was adopted as the primary analytical approach (P<0.05), whereas the remaining methods were applied for sensitivity validation. Furthermore, IVW results with P<0.05 and an FDR-adjusted P-value threshold of <0.2[19-20] were established as heuristics to define evidence for the association between immune cells and PDR. For palindromic A/T and C/G variants, strand orientation was inferred by comparing effect allele frequencies across the two datasets. Palindromic SNPs with insufficient effect allele frequencies differences to resolve strand ambiguity were flagged with mr_keep=FALSE and excluded from subsequent MR analyses. SNPs showing significant associations with candidate genes were selected as IVs (P<1×10^{-5}), and IVs exhibiting linkage disequilibrium were excluded using clumping criteria (clump=TRUE, R^2=0.001, kb=10 000)[21-22]. The F-statistic was computed, and IVs with F-values >10 were retained to avoid bias caused by weak instruments. To satisfy the independence assumption, potential confounding factors associated with the outcomes were screened and excluded using the PhenoScanner system (http://www.phenoscanner.medschl.cam.ac.uk/).

Sensitivity analysis for MR analysis Sensitivity analyses were performed using heterogeneity, horizontal pleiotropy tests, and leave-one-out (LOO) analysis. To assess potential horizontal pleiotropy, Mendelian randomization pleiotropy residual sum and outlier (MR-PRESSO) with MR-Egger regression. MR-PRESSO global test (P<0.05) suggested that causal estimates were distorted by pleiotropic outlier instrumental SNPs. Outliers detected using these methods were iteratively removed until all of the MR-PRESSO global test P>0.05[23]. MR-Egger regression with P>0.05 was applied to assess and exclude potential horizontal pleiotropy for each IV. Cochran's Q statistics and corresponding P-values were applied to evaluate heterogeneity, with P>0.05 indicating the absence of significant heterogeneity effects. When heterogeneity was identified (P<0.05), a random-effects model was employed; otherwise, a fixed-effects model was considered appropriate (P>0.05). Additionally, the LOO approach was performed to evaluate result robustness and determine whether individual SNPs exerted substantial effects on the overall estimates. Forest plots were generated to visualize the analytical results. Steiger's directionality test was applied to rule out reverse causation, by comparing the proportion of variance in exposure versus outcome explained by instrumental variants. Immune cells with an odds ratio (OR) >1 were interpreted as potential risk factors for DR, whereas those with an OR<1 were considered potential protective factors. Scatter plots and funnel plots were further generated to evaluate the stability.

SNP annotation The SNPs were annotated using online tools (https://www.ncbi.nlm.nih.gov/snp/).

Prioritization of Genes by Combining MR with scRNA-seq Results SNPs-annotated genes were mapped to pathways enriched in PDR scRNA-seq datasets. Subsequently, pathways prioritized through annotated genes in the major PDR cell populations were intersected to determine overlapping candidate genes.

Cell Culture and Treatment Human retinal endothelial cells (hRECs) were obtained from BeNa Culture Collection (BNCC340909, Xinyang, China) and cultured in Dulbecco's modified Eagle's medium (DMEM, 1.0 g/L D-glucose; Gibco, USA) comprising 10% fetal bovine serum (FBS; BC-SE-FBS01, Biochannel, Nanjing, China) and 1% penicillin-streptomycin (P/S; SV30010, HyClone, USA). Human monocytic leukemia cell line (THP-1) cells were obtained from the American Type Culture Collection (ATCC, USA) and maintained in RPMI-1640 medium (Sigma-Aldrich, USA) comprising 10% FBS (BC-SE-FBS01, Biochannel, Nanjing, China) and 1% P/S (SV30010, HyClone, USA). To induce differentiation into macrophages, THP-1 monocytes were incubated with phorbol 12-myristate 13-acetate (PMA, 100 ng/mL, HY-18739, MCE, USA).

Cells underwent culture in a humidified incubator containing 5% CO_2 at 37°C. To establish an *in vitro* DR-like inflammatory microenvironment, hRECs and THP-1 cells were exposed for 48h to the following conditions: lipopolysaccharide group (LPS, 2 μg/mL, positive control) and normal control (NC, standard culture media). Cells between passages 3 and 6 were selected for all experiments.

Quantitative Real-Time Polymerase Chain Reaction To validate findings obtained from public database analyses, RNA extraction and quantitative real-time polymerase chain reaction (qRT-PCR) were performed in hRECs and THP-1 cells subjected to LPS group and NC treatments.

Expression levels underwent normalization against actin as the internal reference gene, and relative expression was computed using the $2^{-\Delta\Delta Ct}$ method. Finally, key genes exhibiting consistent expression patterns between qRT-PCR results and the dataset analysis were selected as candidate genes.

Statistical Analysis Statistical analyses were conducted using R software version 4.2.1 and associated R packages. all experiments were performed with at least three independent biological replicates, and each biological sample included three technical replicates to ensure analytical reliability. Data are denoted as mean±standard deviation (SD) from three independent experiments. Statistical analyses were further

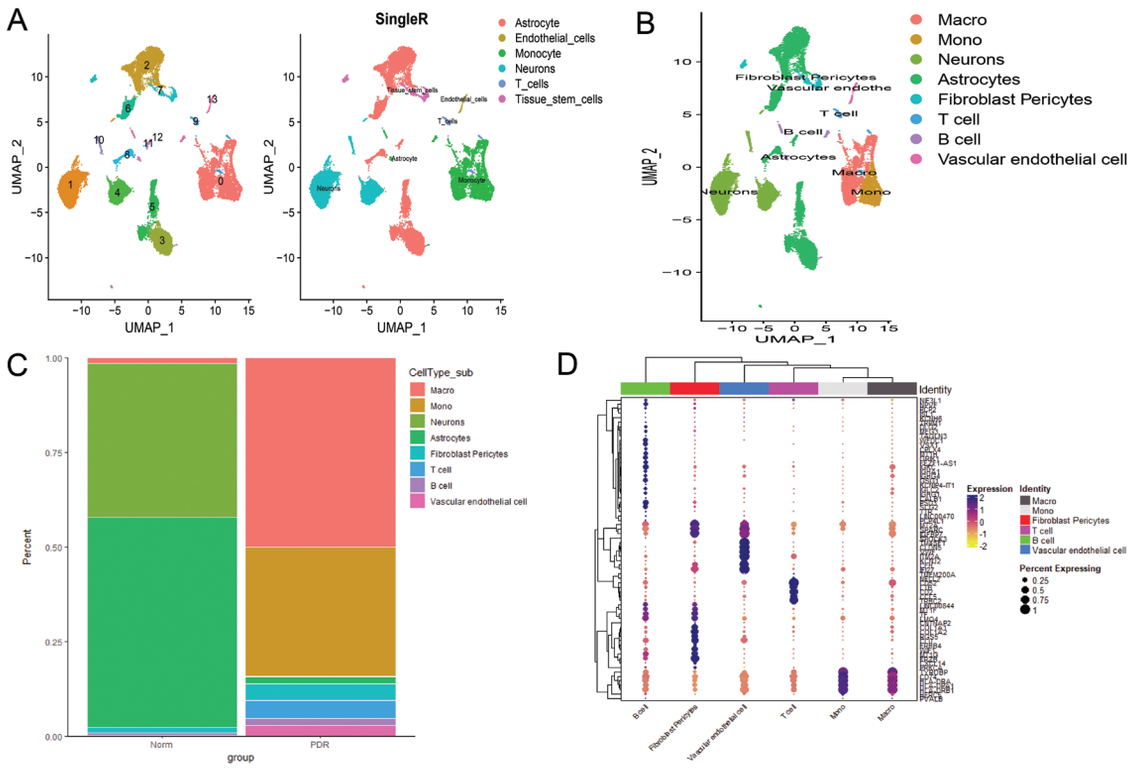


Figure 2 scRNA-seq analysis A: UMAP visualization generated by SingleR based on integrated scRNA-seq datasets; B: UMAP representation of major cell populations identified from integrated scRNA-seq datasets; C: Distribution proportions of annotated cell populations; D: Heatmap illustrating the expression patterns of top marker genes in major cell populations from PDR. PDR: Proliferative diabetic retinopathy; scRNA-seq: Single-cell RNA sequencing; UMAP: Uniform Manifold Approximation and Projection.

executed utilizing GraphPad Prism 10.1 (GraphPad Software, USA). Two-way analysis of variance (ANOVA) was utilized to evaluate differences between LPS and NC treatments in hRECs and THP-1 cells. Subsequently, the Benjamini-Hochberg false FDR method was employed to adjust *P*-values across all analyzed genes, controlling the expected proportion of false positives at FDR<0.05[24]. Statistical significance was defined as FDR<0.05.

RESULTS

Single-Cell Overview of FVMs Cell Compositions

scRNA-seq datasets were obtained from the GEO database (GSE188280, GSE165784). After stringent quality control procedures, all scRNA-seq datasets were integrated and normalized to minimize heterogeneity among different sample groups. This analysis established a comprehensive cellular atlas, in which all cells were classified into 13 distinct clusters (Figure 2A). Dimensionality reduction and visualization of cellular subpopulations were performed using the Uniform Manifold Approximation and Projection (UMAP) method. After data standardization and quality filtering, clustering analysis of the scRNA-seq datasets identified nine predominant cell types, including macrophages, astrocytes, monocytes, vascular endothelial cells, neurons, fibroblasts, pericytes, B cells, and T cells (Figure 2B). Analysis of cellular composition showed that the major cell populations identified in PDR FVMs included macrophages, monocytes, T cells, B cells, retinal vascular endothelial cells, fibroblasts, and pericytes. Among these populations, macrophages, monocytes, and T cells might represent the major pathogenic cell subsets associated with PDR progression (Figure 2C, 2D).

MR Results MR analysis was conducted to assess potential causal relationships between immune cells (monocytes and $CD8^+$ T cells) and PDR. To reduce the likelihood of false-positive findings, the FDR method was applied to adjust *P*-values derived from the IVW analysis. Analysis of the finngen_R9_DM_RETINA_PROLIF dataset further identified three immune cell traits associated with PDR, among which two were considered risk factors. Two immune cell types showed consistent associations with increased PDR risk across the dataset: CD8 on CM CD8br and HLA DR on $CD14^+CD16^-$ monocytes (Figure 3). Subsequent analyses focused on these two immune cell types.

Sensitivity Analysis Sensitivity analyses were conducted on the integrated results from the PDR dataset to evaluate the robustness of the MR findings. Heterogeneity analysis identified no significant differences ($P>0.05$) between the immune cells and PDR (Table 1). The MR-Egger intercept test and MR-PRESSO global test ($P>0.05$) provided no evidence of horizontal pleiotropy, Steiger's test confirmed the expected causal direction from immune traits to PDR, arguing

exposure	nsnp	method	pval	OR(95%CI)
CD8 on CM CD8br	13	Weighted median	0.193	1.055 (0.973 to 1.143)
	13	Inverse variance weighted	**0.012**	1.077 (1.017 to 1.140)
CM CD8br %T cell	20	Weighted median	0.316	0.960 (0.886 to 1.040)
	20	Inverse variance weighted	**0.008**	0.929 (0.880 to 0.981)
HLA DR on CD14+ CD16− monocyte	19	Weighted median	**<0.001**	1.113 (1.061 to 1.167)
	19	Inverse variance weighted	**<0.001**	1.079 (1.034 to 1.126)

Figure 3 Figure map of the MR causal effect between immune cells and PDR PDR: Proliferative diabetic retinopathy; MR: Mendelian randomization; OR: Odds ratio; CI: Confidence interval; nsnp: Number of single nucleotide polymorphisms.

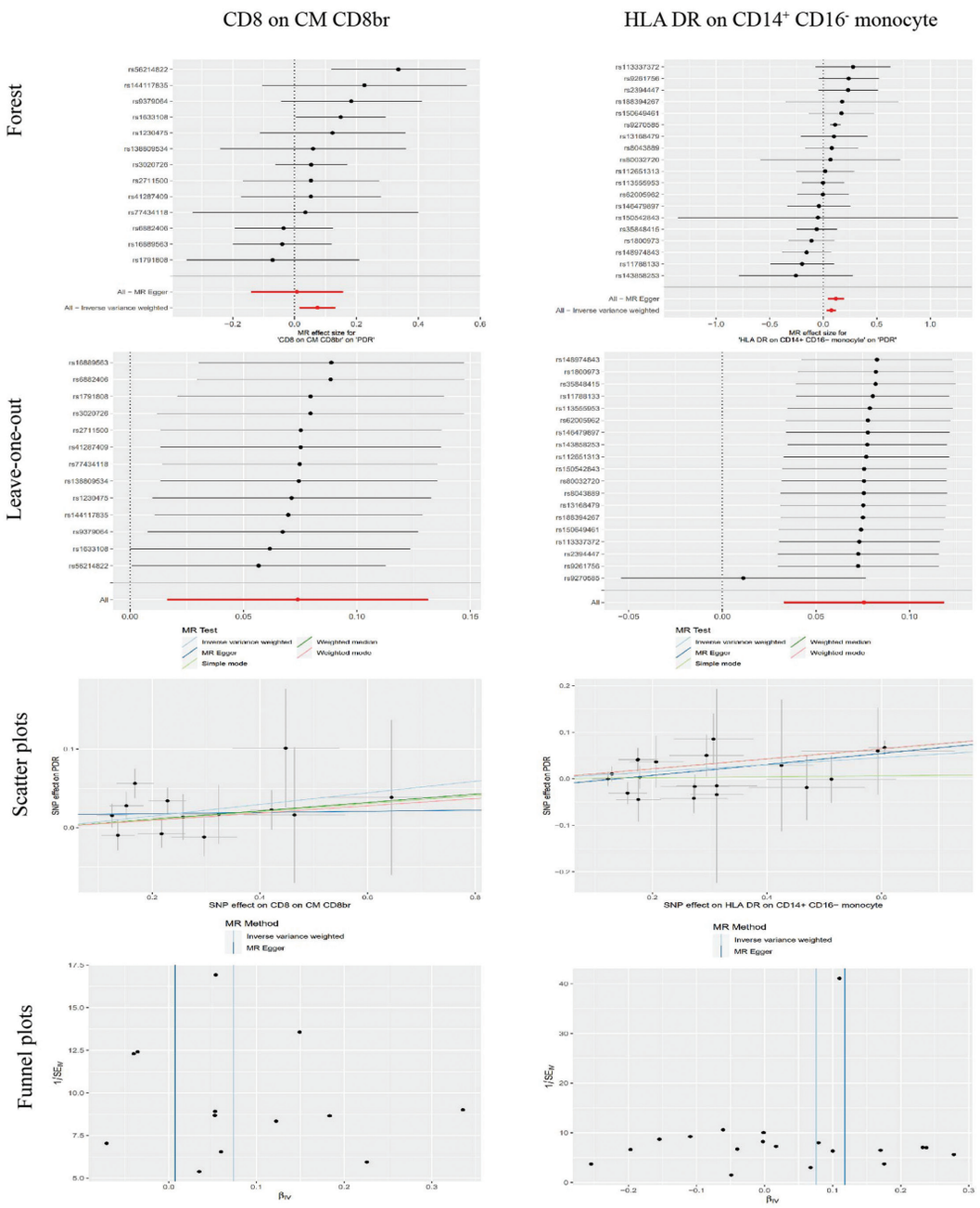


Figure 4 Sensitivity analysis for immune cells and PDR PDR: Proliferative diabetic retinopathy; MR: Mendelian randomization; SNP: Single-nucleotide polymorphism.

against reverse causality (Table 2). LOO sensitivity analysis demonstrated that no single SNP had disproportionately influenced on the overall effect estimate. Furthermore, scatter plots and funnel plots supported the stability of the causal associations between the identified immune cells (CD8 on CM CD8br and HLA DR on $CD14^{+}CD16^{-}$ monocytes) and PDR (Figure 4).

SNPs Annotation and Pathways in Cells with the Major Cell Populations of PDR The 13 SNPs in immune cells (CD8 on CM CD8br) exhibited strong associations with

Table 1 Heterogeneity test of PDR and immune cells

Outcome	Exposure	Method	*Q*	*Q*_df	*Q*_pval
PDR	CD8 on CM CD8br	MR Egger	12.512	11	0.326
PDR	CD8 on CM CD8br	IVW	13.544	12	0.331
PDR	HLA DR on $CD14^+CD16^-$ monocyte	MR Egger	19.883	17	0.280
PDR	HLA DR on $CD14^+CD16^-$ monocyte	IVW	21.994	18	0.232

PDR: Proliferative diabetic retinopathy; MR-Egger: Mendelian randomization-Egger; IVW: Inverse-variance weighted.

Table 2 Horizontal pleiotropy test of PDR and immune cells

Outcome	Exposure	Egger_intercept	SE	*P*	MR-PRESSO global *P*	Correct_causal direction	Steiger *P*
PDR	CD8 on CM CD8br	0.016	0.017	0.361	0.314	TRUE	0
PDR	HLA DR on $CD14^+CD16^-$ monocyte	-0.016	0.012	0.197	0.241	TRUE	0

PDR: Proliferative diabetic retinopathy; SE: Standard error; MR-PRESSO: Mendelian randomization pleiotropy residual sum and outlier.

the PDR dataset, while 19 SNPs were identified in immune cells (HLA DR on $CD14^+CD16^-$ monocytes). Shared SNPs between the two immune cell groups that showed significant associations with the PDR dataset were annotated, prioritizing candidate genes potentially involved in PDR, including *ZMAT4*, *ZBTB16*, *PIP5K1B*, and *CD8A* in CD8 on CM CD8br, as well as *GLI2*, *KATNIP*, *LYZ*, *ERBB4*, *UQCC2*, *WDR72*, *RYR2*, *ZNF442*, and *FLJ12825* in HLA DR on $CD14^+CD16^-$ monocytes. Subsequently, GSEA was performed to characterize enriched pathways in the major cell populations of PDR. Several immune-related pathways were identified among the pathways enriched in PDR-associated cells (Figure 5). Further analysis demonstrated that *CD8A* (rs3020726 annotation) was mapped in the HALLMARK_ALLOGRAFT_REJECTION immune pathway of T cells, whereas *ZBTB16* (rs1791808 annotation) was enriched in the HALLMARK_P53_PATHWAY of macrophages and in the HALLMARK_KRAS_SIGNALING_DN of macrophages and fibroblasts_pericytes. The HALLMARK_ALLOGRAFT_REJECTION pathway showed enrichment across the major cell populations in patients with PDR. In contrast, the HALLMARK_P53_PATHWAY was downregulated in macrophages (NES=-1.506; *Q*-value=0.018; *P*=0.005); the HALLMARK_KRAS_SIGNALING_DN pathway was downregulated in macrophages (NES=-1.722; *Q*-value=0.008; *P*=0.002) and fibroblasts_ pericytes (NES=-1.156; *Q*-value=0.219; *P*=0.243).

Prioritization of Candidate Genes by qRT-PCR The HALLMARK_ALLOGRAFT_REJECTION gene set showed positive enrichment across the major cell populations (Figure 6). Enrichment remained significant in macrophages (NES=1.458, FDR=0.018), fibroblast_pericyte populations (NES=2.139, FDR<0.001), and B cells (NES=2.733, FDR<0.001). Positive but non-FDR-significant enrichment was observed in monocytes (NES=1.653, FDR=0.082), T cells (NES=1.563, FDR=0.074), and vascular endothelial cells (NES=1.278, FDR=0.294). Subsequently, genes involved in this pathway among these cell populations were intersected using Jvenn[25], prioritizing six overlapping genes (*CTSS*, *STAT1*, *B2M*, *CD74*, *CCL2*, *TIMP1*). However, *CTSS* was the only leading-edge gene shared across all six cell types (Figure 7A). We therefore selected *CTSS* for experimental validation using an inflammatory microenvironment model of DR. qRT-PCR analysis assayed that *CTSS* expression was significantly upregulated in LPS-stimulated THP-1 cells, consistent with the dataset findings; however, no statistically significant difference in *CTSS* expression was detected between the LPS and control groups in hRECs (Figure 7B).

DISCUSSION

Accumulating evidence indicates that immune dysregulation and inflammatory responses are closely involved in the pathogenesis of DR. Previous MR analyses have prioritized causal associations between several immune cell traits and DR[9-10]. However, these investigations did not specifically distinguish DR from PDR when evaluating immune cell-related effects. Previous studies have demonstrated that M1 polarization, monocytes, and $CD8^+$ T cells contribute to PDR development through complex cellular interactions. The present study integrated MR analysis of these three immune cell types with PDR-related scRNA-seq data derived from FVMs of patients with PDR to prioritize novel immune-related candidate genes and pathways associated with the diagnosis and treatment of PDR for further investigation.

The present study focused on the contributions of M1 polarization, monocytes, and $CD8^+$ T cells to PDR by systematically reviewing the literature regarding the functions of 731 immune cell types. Specific monocyte and $CD8^+$ T cell subsets associated with macrophage M1 phenotype polarization were identified, and their potential causal associations with PDR were further evaluated. Among the 731 immune cell types analyzed, 139 were $CD8^+$ T cell subsets, and 63 were monocyte subsets. Among these populations, only 24 $CD8^+$ T-cell subsets and 9 monocyte subsets (specifically $CD14^+CD16^-$ monocytes) showed explicit associations with M1 macrophages. Distinct immune cell subsets exert different regulatory effects: $CD8^+$ T

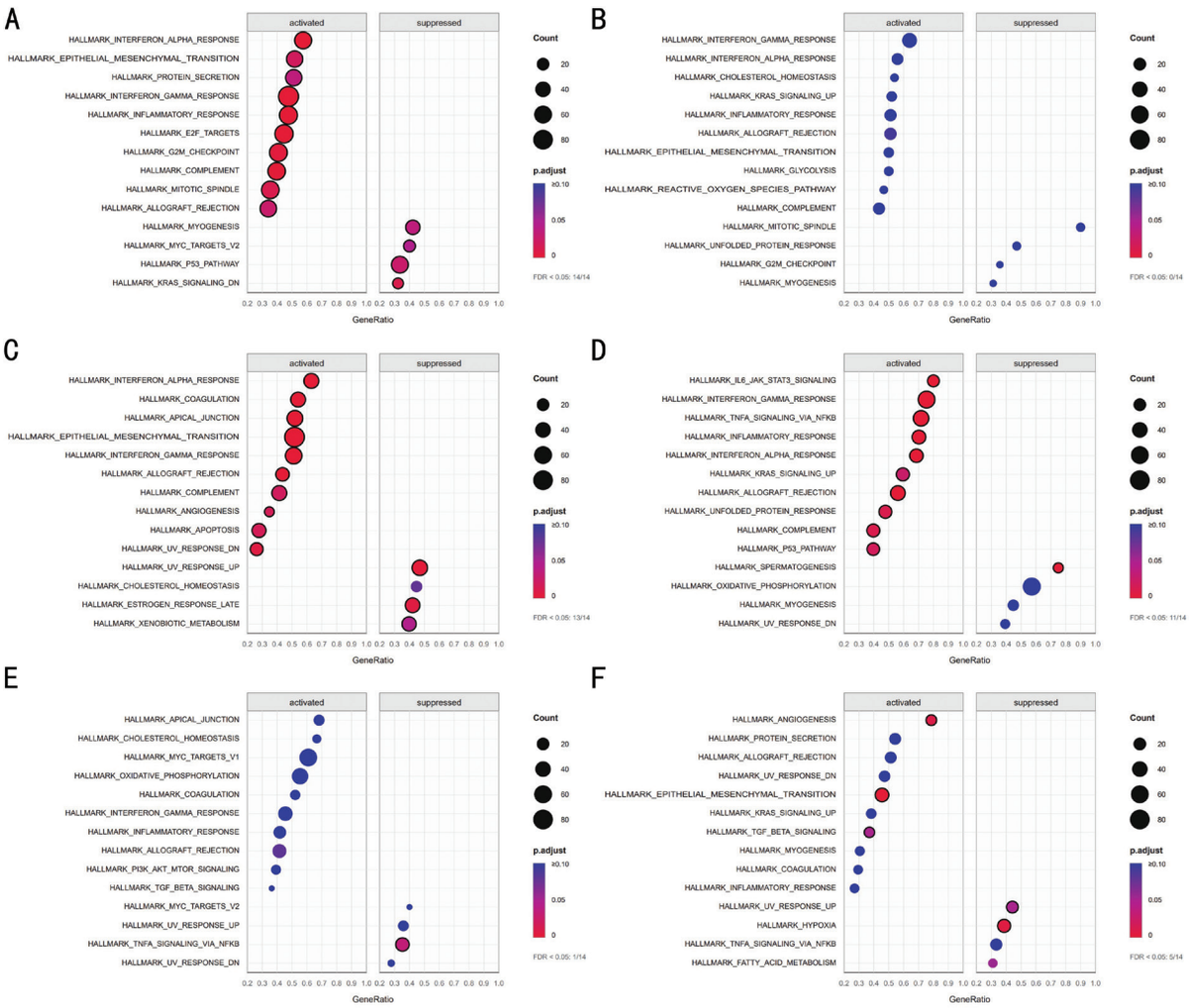


Figure 5 Several immune-related pathways are present in the major cell populations of PDR A: Macrophages; B: Monocytes; C: Fibroblast pericytes; D: B cells; E: T cells; F: Vascular endothelial cells. PDR: Proliferative diabetic retinopathy; FDR: False discovery rate.

cell subsets (CD8br and $CD45RA^{+}CD28^{-}$) enhance immune activation through elevated IFN-γ secretion, thereby promoting M1 polarization[15-17]. In contrast, immune populations that do not induce M1 polarization, suppress this process, or favor macrophage M2 polarization include $CD8^{+}$ T cells ($CD4^{-}CD8^{-}$), also referred to as double-negative (DN) T cells, which may exhibit characteristics of inducible regulatory T cells (Tregs)[26]; regulatory $CD8^{+}$ T cells defined as $CD8^{+}CD25^{++}$[27]; and regulatory T-cell subsets characterized by $CD8^{+}CD28^{-}CD127^{-}CD39^{+}$[28]. Monocytes are recruited to specific vascular or tissue sites through chemokine-mediated signaling and receptor interactions, where they differentiate into macrophages following tissue injury or infection[29]. Three major monocyte subsets have been characterized: classical ($CD14^{+}CD16^{-}$), intermediate ($CD14^{+}CD16^{+}$), and nonclassical ($CD14^{-}CD16^{+}$). Classical monocytes can differentiate into macrophages within tissues and contribute to chronic disease[13], whereas nonclassical monocytes generally exhibit limited differentiation into macrophages under homeostatic conditions[30]. Finally, MR analysis demonstrated potential causal associations between immune cells and PDR, indicating that CD8 on CM CD8br and HLA DR on $CD14^{+}CD16^{-}$ monocytes were associated with increased PDR risk.

This study investigated the potential effects of immune-related candidate genes and pathways on PDR progression. scRNA-seq of FVMs from patients with PDR revealed that the major cellular components include macrophages, monocytes, T cells, B cells, retinal vascular endothelial cells, fibroblasts, and pericytes. Our study indicated that macrophages, monocytes, and T cells constitute the predominant cell populations in FVMs, further validating the biological significance of immune cells, particularly monocytes and $CD8^{+}$ T cells. Among the pathways enriched in PDR-associated cells, several immune-related pathways were identified. SNP annotation further prioritized genes potentially involved in PDR pathogenesis. Subsequent analysis demonstrated that ZBTB16 was enriched in the HALLMARK_P53_PATHWAY, displaying selective enrichment in macrophages but reduced pathway activity. The MSigDB Hallmark collection[31] categorizes the HALLMARK_P53_PATHWAY within the

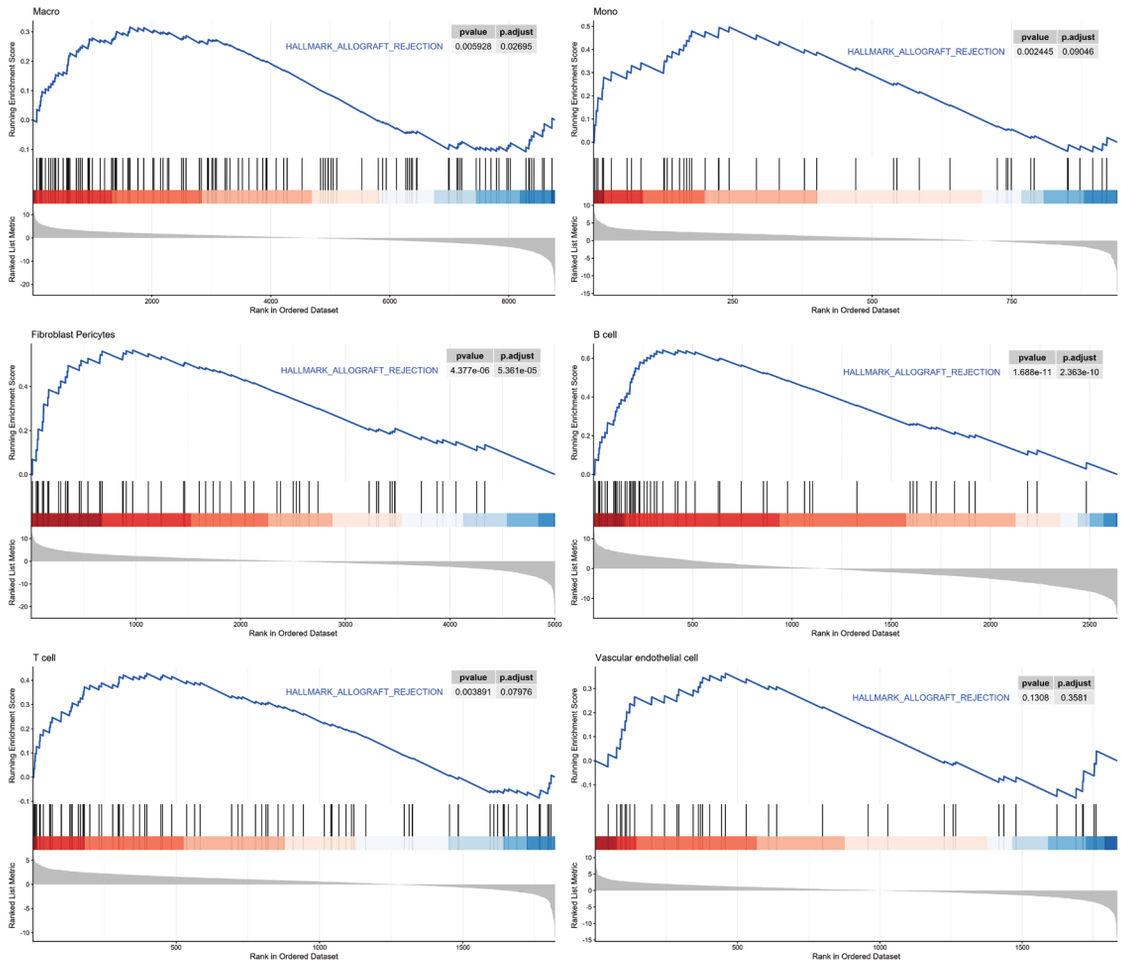


Figure 6 The HALLMARK_ALLOGRAFT_REJECTION pathway of the major cell populations in PDR PDR: Proliferative diabetic retinopathy.

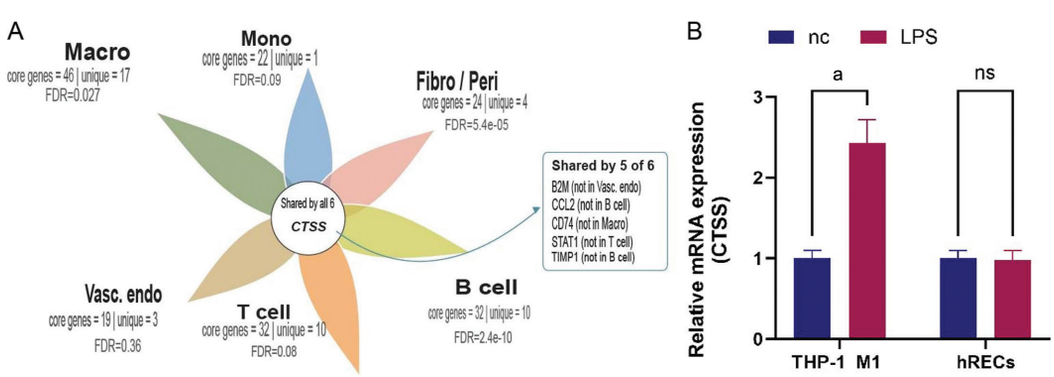


Figure 7 Prioritization of immune-related candidate genes in an inflammatory microenvironment model of DR A: *CTSS* were identified the only leading-edge gene shared across all six cell types; B: Expression levels of the *CTSS* genes were determined by qRT-PCR in the THP-1 cells and hRECs in an inflammatory microenvironment model. DR: Diabetic retinopathy; hREC: Human retinal endothelial cells; qRT-PCR: Quantitative real-time polymerase chain reaction; THP-1: Human monocytic leukemia cell line; ns: Not significant; LPS: Lipopolysaccharide. [a]*P*<0.0001.

proliferation-related process group, with major biological functions involving cell cycle arrest, DNA damage repair, and apoptosis. The reduced activity of the HALLMARK_P53_PATHWAY in FVM-derived macrophages may be maintained within the proinflammatory microenvironment. HALLMARK_KRAS_SIGNALING_DN (MSigDB ID: M5956) is a hallmark transcriptional signature comprising 200 genes that are repressed upon KRAS activation[31]. Importantly, the directionality of this gene set must be carefully considered: its member genes are transcriptionally suppressed when KRAS signaling is activated. Therefore, relative downregulation (or a negative NES) of this gene set in our results indicates elevated KRAS-MAPK pathway activity. Previous studies have shown that enrichment or suppression patterns of HALLMARK_KRAS_SIGNALING_DN are associated with molecular subtypes and prognosis in multiple cancers[32]. Currently, there

is limited research on the role of this pathway in PDR, further more studies are needed.

However, CD8A was mapped in the HALLMARK_ALLOGRAFT_REJECTION immune pathway, which showed positive enrichment across the major cell populations from patients with PDR. Enrichment remained significant in macrophages, fibroblast_pericyte, and B cells. Positive but non-FDR-significant enrichment was observed in monocytes, T cells, and vascular endothelial cells. The HALLMARK_ALLOGRAFT_REJECTION gene set broadly represents immune activation and antigen presentation pathways; in this study, there is currently no definitive evidence that this pathway constitutes a specific pathogenic mechanism for DR. However, it has been reported to correlate strongly with infiltration of antitumor immune populations, including $CD8^+$ T cells, $CD4^+$ memory T cells, M1 macrophages, and plasmacytoid dendritic cells (pDC)[33], which is consistent with the findings of the present study. Subsequently, genes involved in this pathway among these cell populations were intersected and prioritized six overlapping genes (*CTSS*, *STAT1*, *B2M*, *CD74*, *CCL2*, *TIMP1*). In DR, STAT1 has been reported to promote microglial cuproptosis through regulation of SLC31A1 expression, thereby aggravating retinal inflammation[34]. Exosomal microRNA-17-3p derived from human umbilical cord mesenchymal stem cells alleviated oxidative stress, suppressed retinal cell apoptosis, and decreased inflammatory cytokine and VEGF production by inhibiting STAT1 activity[35]. Under high glucose conditions, STAT1 regulated Bim expression and promoted retinal pericyte apoptosiss[36]. β-2-Microglobulin, encoded by *B2M*, is a small component of the major histocompatibility class I molecule and is expressed on all nucleated cells. B2M has been proposed as an early biomarker and potential therapeutic target for diabetic kidney disease accompanied by DR[37]. Tear proteomic analysis in patients with DR demonstrated increased B2M levels in individuals with NPDR compared with healthy controls, suggesting its potential application as an early biomarker for DR[38]. CD74 is the major histocompatibility class II-associated invariant chain[39]. Western blot analysis demonstrated significantly increased CD74 expression on stromal cell membranes from patients with active PDR compared with those with inactive PDR. Additionally, vitreous samples from patients with PDR exhibited markedly higher CD74 protein levels than those from non-diabetic controls. These observations suggest that the MIF/CD74 signaling pathway may contribute to PDR angiogenesis and progression, representing a potential therapeutic target for vascular dysfunction in PDR[40]. Furthermore, diabetic rat studies have identified CD74 as a marker associated with microglial activation in the diabetic retina[41]. Matrix metalloproteinases are involved in DR pathogenesis, whereas TIMP1 functions as a potent endogenous inhibitor of most matrix metalloproteinases[42]. The chemokine CCL2, commonly known as monocyte chemoattractant protein-1 (MCP-1), has been found to be significantly elevated in the vitreous humor of patients with PDR[43]. Due to its ability to induce leukocyte migration and promote chronic retinal inflammation, MCP-1 is considered to play a pivotal role in the pathogenesis of DR[44]. A prospective complication study based on plasma samples from 493 patients with type 1 diabetes enrolled in the Prospective Complications Study (EURODIAB) trial demonstrated an association between elevated TIMP1 levels and PDR. Compared with patients without retinopathy, individuals with PDR exhibited significantly higher TIMP1 concentrations, whereas no significant association was observed in patients with NPDR[45]. During intraocular surgery, aqueous humor samples were collected from healthy controls and patients with non-apparent DR, mild/moderate NPDR, and advanced NPDR/PDR. The analysis demonstrated significantly elevated TIMP1 levels in the aqueous humor of patients with advanced NPDR and PDR[46]. Among these overlapping genes, CTSS was the only leading-edge gene shared across all six cell types. CTSS is a lysosomal protease involved in intracellular protein degradation, extracellular matrix remodeling, and major histocompatibility complex class II antigen processing and presentation[47]. CTSS is mainly expressed by macrophages and dendritic cells[48]. The involvement of CTSS has been investigated in several ocular disease models. The LINC02099/miRNA-214-3p/CTSS axis regulates extracellular matrix-related gene expression in Müller cells and contributes to retinal fibrosis in diabetic mice[49]. In a choroidal neovascularization mouse model, CTSS deficiency reduced inflammatory signaling and attenuated angiogenic responses[50]. Previous studies have indicated that CTSS inhibition may suppress inflammatory activity, mitigate microvascular injury, and limit angiogenesis under hyperglycemic conditions[51]. In our study, macrophages were the predominant cell population in FVMs, *CTSS* expression was significantly upregulated in LPS-stimulated THP-1 cells, which served as an inflammatory microenvironment model of DR. *CTSS* may be a potential pathogenic gene in PDR, we hope to explore innovative research methods to provide new strategies for multi-target synergistic therapy in patients with PDR.

However, several limitations should be acknowledged in this study. First, the MR findings were derived from bioinformatics analyses of publicly available databases and were primarily based on European populations, which may restrict their generalizability to other ethnic groups. Second, PDR data were obtained from the R9 dataset of the FinnGen database because the R10 dataset is no longer maintained, while R11 and R12

do not provide independent PDR datasets. Nevertheless, the scRNA-seq dataset was generated from FVMs of patients with PDR. Therefore, the use of the R9 dataset is unlikely to compromise the investigation of immune mechanisms involved in PDR. Third, the 731 immune cell phenotypes represent diverse characteristics related to surface marker expression and cellular proportions. These phenotypes were obtained from the IEU OpenGWAS database, which is based on peripheral blood flow cytometry GWAS cohorts and reflects circulating immune profiles rather than tissue-resident immune populations within PDR FVMs. Therefore, certain weak but genuine causal associations may have been overlooked due to stringent multiple-testing corrections. Therefore, monocyte and $CD8^+$ T cell subsets were prioritized based on their identified potential causal associations. Although a relatively relaxed threshold ($P<1\times10^{-5}$) was applied, additional strategies, including sensitivity analyses and *P*-value correction approaches, were implemented to evaluate the biological plausibility of selected IVs. These complementary analyses aimed to achieve an appropriate balance between statistical power and biological relevance. Further investigations will be required when more robust and suitable datasets become available. Moreover, collaborative efforts are encouraged to establish improved strategies for addressing the challenges associated with balancing data availability and biological interpretation. Additionally, scRNA-seq analysis used normal retinal scRNA-seq data as a reference framework for characterizing cellular heterogeneity within PDR FVMs. Lam *et al*[52] reported that postmortem retinas were used to define expression baseline because there is no normal correlate of FVMs. However, these tissues differ from FVMs in certain biological and anatomical characteristics. Future studies should incorporate additional control tissues with closer pathological and biological relevance to facilitate more rigorous comparative analyses. Additionally, the limited number of donor samples results in low statistical power and may yield unreliable results. Therefore, these results are exploratory and require confirmation using donor-aware methods in larger cohorts. Fourth, validation was performed only at the genetic level using an inflammatory microenvironment model of DR. Future validation studies involving FVMs, vitreous samples, and osmotic pressure-related factors are expected to provide further evidence and improve the robustness of the findings. Finally, the scRNA-seq datasets were exclusively derived from FVM samples of patients with PDR, and the MR outcome datasets were also specific to PDR, limiting the ability to assess early-stage DR pathogenesis. Despite these limitations, this study primarily aims to prioritize potential research directions rather than establish definitive conclusions, providing additional insights into immune-related mechanisms associated with PDR.

In conclusion, this study prioritizes immune-related candidate genes and pathways potentially involved in PDR pathogenesis, providing new insights for further investigation.

ACKNOWLEDGEMENTS

This study was based on publicly accessible datasets. Appreciation is extended to the researchers contributing to the GEO, FinnGen, and IEU GWAS projects, whose efforts enabled the generation and availability of these valuable resources.

Authors' Contributions: Gao Y and Yan F contributed primarily to the experimental design, manuscript revision, data analysis and interpretation, and preparation of the manuscript. Wang JF performed hRECs and THP-1 cells culture and related cell experiments. Deng JY, Ge PF, and Lin YF contributed to data acquisition and statistical analyses. Lu YY and Xie HY contributed to data visualization. As corresponding authors, Hu ZZ and Xie P critically evaluated, revised, and approved the final manuscript. All authors have read and approved the final version of the manuscript.

Data Availability Statement: The scRNA-seq datasets (GSE188280 and GSE165784) analyzed in this study are available from the GEO repository (https://www.ncbi.nlm.nih.gov/geo/). GWAS summary statistics for PDR were obtained from the FinnGen R9 database (https://www.finngen.fi/). Additionally, immune cell-related data were retrieved from the IEU Open GWAS project (https://gwas.mrcieu.ac.uk/).

AI-Generated Content Disclosure: No artificial intelligence (AI) tools or large language models were used in the writing, analysis, or generation of any content in this manuscript.

Foundations: Supported by the National Natural Science Foundation of China (No.82371076; No.82471095); the Medical-Engineering Interdisciplinary Translational Fund of the First Affiliated Hospital of Nanjing Medical University (No.QG202405).

Conflicts of Interest: Gao Y, None; **Yan F,** None; **Wang JF,** None; **Deng JY,** None; **Ge PF,** None; **Lin YF,** None; **Lu YY,** None; **Xie HY,** None; **Hu ZZ,** None; **Xie P,** None.

REFERENCES

1 Gbd B, Collaborators VI, Vision Loss Expert Group of the Global Burden of Disease Study. Causes of blindness and vision impairment in 2020 and trends over 30 years, and prevalence of avoidable blindness in relation to VISION 2020: the Right to Sight: an analysis for the Global Burden of Disease Study. *The Lancet Glob Heal* 2021;9(2):e144-e160.

2 Gauldin D, Ahmad KT, Ferguson S, *et al*. Exposure of contralateral eyes to laser radiation during retinal photocoagulation. *Curr Eye Res* 2021;46(9):1424-1427.

3 Suresh R, Yu HJ, Thoveson A, *et al*. Loss to follow-up among patients with proliferative diabetic retinopathy in clinical practice. *Am J Ophthalmol* 2020;215:66-71.

4 Pearce E, Chong V, Sivaprasad S. Aflibercept reduces retinal hemorrhages and intravitreal microvascular abnormalities but not venous beading: secondary analysis of the CLARITY study. *Ophthalmol Retina* 2020;4(7):689-694.

5 Davies NM, Holmes MV, Davey Smith G. Reading Mendelian randomisation studies: a guide, glossary, and checklist for clinicians. *BMJ* 2018;362:k601.

6 Cheng CD, Chen WA, Jin HJ, *et al*. A review of single-cell RNA-seq annotation, integration, and cell-cell communication. *Cells* 2023;12(15):1970.

7 Tang CY, Yang YQ, Liang YB, *et al*. Mendelian randomization analysis of causal relationship between cheese intake and diabetic retinopathy. *Int J Ophthalmol* 2024;17(10):1905-1910.

8 Pan WW, Lin F, Fort PE. The innate immune system in diabetic retinopathy. *Prog Retin Eye Res* 2021;84:100940.

9 Ye YY, Dai L, Gu H, *et al*. The causal relationship between immune cells and diabetic retinopathy: a Mendelian randomization study. *Front Immunol* 2024;15:1381002.

10 Li YY, Xiang Y, Mou B, *et al*. Causal influence of immune factors on the risk of diabetic retinopathy: a Mendelian randomization study. *Diabetol Metab Syndr* 2024;16(1):194.

11 Gao N, Hao SL, Huang GN, *et al*. The integrated transcriptome bioinformatics analysis identifies key genes and cellular components for proliferative diabetic retinopathy. *PLoS One* 2022;17(11):e0277952.

12 Yao YJ, Li JJ, Zhou YF, *et al*. Macrophage/microglia polarization for the treatment of diabetic retinopathy. *Front Endocrinol (Lausanne)* 2023;14:1276225.

13 Narasimhan PB, Marcovecchio P, Hamers AAJ, *et al*. Nonclassical monocytes in health and disease. *Annu Rev Immunol* 2019;37:439-456.

14 Huang J, Zhou Q. $CD8^+$ T cell-related gene biomarkers in macular edema of diabetic retinopathy. *Front Endocrinol* 2022;13:907396.

15 Sharma N, Fan XZ, Atolagbe OT, *et al*. ICOS costimulation in combination with CTLA-4 blockade remodels tumor-associated macrophages toward an antitumor phenotype. *J Exp Med* 2024;221(4): e20231263.

16 Kusaka Y, Kajiwara C, Shimada S, *et al*. Potential role of Gr-1^+ $CD8^+$ T lymphocytes as a source of interferon-γ and M1/M2 polarization during the acute phase of murine legionella pneumophila pneumonia. *J Innate Immun* 2018;10(4):328-338.

17 Doan Ngoc TM, Tilly G, Danger R, *et al*. Effector memory–expressing CD45RA (TEMRA) $CD8^+$ T cells from kidney transplant recipients exhibit enhanced purinergic P2X4 receptor–dependent proinflammatory and migratory responses. *J Am Soc Nephrol* 2022;33(12):2211-2231.

18 Pan ZH, Zhang MD, Zhang FY, *et al*. Single-cell transcriptomics unveils the dedifferentiation mechanism of lung adenocarcinoma stem cells. *Int J Mol Sci* 2023;24(1):482.

19 Huang Y, Wang HX, Zheng JY, *et al*. Relationship of metabolites and metabolic ratios with schizophrenia: a Mendelian randomization study. *Ann Gen Psychiatry* 2024;23(1):34.

20 Zheng Z, Chen DH, Lv JM, *et al*. Causal effects of plasma metabolites on autoimmune hepatitis (AIH): a bidirectional two-sample Mendelian randomization study. *Sci Rep* 2024;14:22944.

21 Song ZW, Li WY, Han YP, *et al*. Association of immune cell traits with Parkinson's disease: a Mendelian randomization study. *Front Aging Neurosci* 2024;16:1340110.

22 Han S, Gao JP, Wang Z, *et al*. Genetically supported causality between gut microbiota, immune cells and morphine tolerance: a two-sample Mendelian randomization study. *Front Microbiol* 2024;15:1343763.

23 Wan HY, Zhong L, Su J, *et al*. Potential risk of cutaneous melanoma attributable to medication use: a Mendelian randomization approach. *Biomedicines* 2025;13(10):2477.

24 Noble WS. How does multiple testing correction work? *Nat Biotechnol* 2009;27(12):1135-1137.

25 Bardou P, Mariette J, Escudié F, *et al*. Jvenn: an interactive Venn diagram viewer. *BMC Bioinformatics* 2014;15(1):293.

26 Velikkakam T, Gollob KJ, Dutra WO. Double-negative T cells: setting the stage for disease control or progression. *Immunology* 2022;165(4):371-385.

27 Gao ML, Liu YL, Guo MQ, *et al*. Regulatory $CD4^+$ and $CD8^+$ T cells are negatively correlated with $CD4^+/CD8^+$ T cell ratios in patients acutely infected with SARS-CoV-2. *J Leukoc Biol* 2021;109(1):91-97.

28 Fenoglio D, Belgioia L, Parodi A, *et al*. Development of exhaustion and acquisition of regulatory function by infiltrating $CD8^+CD28^-$ T lymphocytes dictate clinical outcome in head and neck cancer. *Cancers* 2021;13(9):2234.

29 Medrano-Bosch M, Simón-Codina B, Jiménez W, *et al*. Monocyte-endothelial cell interactions in vascular and tissue remodeling. *Front Immunol* 2023;14:1196033.

30 Hanna RN, Carlin LM, Hubbeling HG, *et al*. The transcription factor NR4A1 (Nur77) controls bone marrow differentiation and the survival of $Ly6C^-$ monocytes. *Nat Immunol* 2011;12(8):778-785.

31 Liberzon A, Birger C, Thorvaldsdóttir H, *et al*. The Molecular Signatures Database (MSigDB) hallmark gene set collection. *Cell Syst* 2015;1(6):417-425.

32 Klomp JA, Klomp JE, Stalnecker CA, *et al*. Defining the KRAS- and ERK-dependent transcriptome in KRAS-mutant cancers. *Science* 2024;384(6700):eadk0775.

33 Oshi M, Patel A, Wu RR, *et al*. Enhanced immune response outperform aggressive cancer biology and is associated with better survival in triple-negative breast cancer. *NPJ Breast Cancer* 2022;8(1):92.

34 Hu Q, Zhang X, Huang JY, *et al*. The STAT1-SLC31A1 axis: potential regulation of cuproptosis in diabetic retinopathy. *Gene* 2024;930:148861.

35 Li W, Jin LY, Cui YB, *et al*. Human umbilical cord mesenchymal stem cells-derived exosomal microRNA-17-3p ameliorates inflammatory reaction and antioxidant injury of mice with diabetic retinopathy *via* targeting STAT1. *Int Immunopharmacol* 2021;90:107010.

36 Shin ES, Huang Q, Gurel Z, *et al*. STAT1-mediated Bim expression promotes the apoptosis of retinal pericytes under high glucose conditions. *Cell Death Dis* 2014;5(1):e986.

37 Fan XE, Xu MH, Chen X, *et al*. Proteomic profiling and correlations with clinical features reveal biomarkers indicative of diabetic retinopathy with diabetic kidney disease. *Front Endocrinol (Lausanne)* 2022;13:1001391.

38 Kim HJ, Kim PK, Yoo HS, *et al*. Comparison of tear proteins between healthy and early diabetic retinopathy patients. *Clin Biochem* 2012;45(1-2):60-67.

39 Leng L, Metz CN, Fang Y, *et al*. MIF signal transduction initiated by binding to CD74. *J Exp Med* 2003;197(11):1467-1476.

40 Abu El-Asrar AM, Ahmad A, Siddiquei MM, *et al*. The proinflammatory and proangiogenic macrophage migration inhibitory factor is a potential regulator in proliferative diabetic retinopathy. *Front Immunol* 2019;10:2752.

41 Wang J, Lin JH, Schlotterer A, *et al*. CD74 indicates microglial activation in experimental diabetic retinopathy and exogenous methylglyoxal mimics the response in normoglycemic retina. *Acta Diabetol* 2014;51(5):813-821.

42 Jayashree K, Yasir M, Senthilkumar GP, *et al*. Circulating matrix modulators (MMP-9 and TIMP-1) and their association with severity of diabetic retinopathy. *Diabetes Metab Syndr Clin Res Rev* 2018;12(6):869-873.

43 Fukutsu K, Murata M, Kikuchi K, *et al*. Acrolein promotes retinal inflammation through macrophage chemotaxis by inducing CCL2 production from Müller cells. *FASEB J* 2026;40(1):e71403.

44 Kovoor E, Chauhan SK, Hajrasouliha A. Role of inflammatory cells in pathophysiology and management of diabetic retinopathy. *Surv Ophthalmol* 2022;67(6):1563-1573.

45 Peeters SA, Engelen L, Buijs J, *et al*. Erratum to: Plasma levels of matrix metalloproteinase-2,-3,-10, and tissue inhibitor of metalloproteinase-1 are associated with vascular complications in patients with type 1 diabetes: the EURODIAB Prospective Complications Study. *Cardiovasc Diabetol* 2015;14:128.

46 Saucedo L, Pfister IB, Zandi S, *et al*. Ocular TGF-β, matrix metalloproteinases, and TIMP-1 increase with the development and progression of diabetic retinopathy in type 2 diabetes mellitus. *Mediators Inflamm* 2021;2021:9811361.

47 Zuo T, Xie Q, Liu JF, *et al*. Macrophage-derived cathepsin S remodels the extracellular matrix to promote liver fibrogenesis. *Gastroenterology* 2023;165(3):746-761.e16.

48 Brown R, Nath S, Lora A, *et al*. Cathepsin S: investigating an old player in lung disease pathogenesis, comorbidities, and potential therapeutics. *Respir Res* 2020;21(1):111.

49 He ZJ, Peng XJ, Feng YQ, *et al*. LINC02099 promotes retinal extracellular matrix deposition in diabetic mice *via* the miRNA-214-3p/CTSS axis. *Invest Ophthalmol Vis Sci* 2025;66(12):42.

50 Preya UH, Sayed S, Nguyen NL, *et al*. Potential role of CTSS in AMDImmune modulatory and anti-angiogenic effects of cathepsin S knockdown in ARPE-19 cells. *Exp Eye Res* 2024;245:109981.

51 Sayed S, Faruq O, Preya UH, *et al*. Cathepsin S knockdown suppresses endothelial inflammation, angiogenesis, and complement protein activity under hyperglycemic conditions *in vitro* by inhibiting NF-κB signaling. *Int J Mol Sci* 2023;24(6):5428.

52 Lam JD, Oh DJ, Wong LL, *et al*. Identification of RUNX1 as a mediator of aberrant retinal angiogenesis. *Diabetes* 2017;66(7):1950-1956.